Photochemical & Photobiological Sciences

Dynamic Article Links

Cite this: *Photochem. Photobiol. Sci.*, 2012, **11**, 1041

www.rsc.org/pps

PAPER

Formation of hydrogen peroxide by VUV-photolysis of water and aqueous solutions with methanol†

Simone Robl,‡[a] Michael Wörner,§[a] Dietrich Maier[b] and André M. Braun¶*[a]

Received 15th November 2011, Accepted 16th February 2012
DOI: 10.1039/c2pp05381k

The hydrogen peroxide production upon vacuum ultraviolet (VUV) irradiation of water is reviewed, because published results from the last 10 years lead to conflicting mechanistic interpretations. This work confirms that in pure water, hydrogen peroxide is only produced in the presence of molecular oxygen. Mechanistic schemes explain these findings and confirm earlier statements that recombination of hydroxyl radicals is kinetically disfavoured. In agreement with other recent publications, this work confirms that enhanced hydrogen peroxide production takes place upon VUV irradiation of aqueous solutions of organic compounds. For these investigations, methanol was chosen as an organic model compound. During photolyses, hydrogen peroxide, dissolved molecular oxygen, pH-value of the reaction system, methanol and its products of oxidative degradation were analyzed, and kinetic studies were undertaken to explain the evolution of the concentrations of these components.

Introduction

VUV-irradiation was found to be highly efficient for the oxidative degradation of organic compounds dissolved or dispersed in condensed aqueous[1] and in gaseous reaction systems.[2] Two lines of excitation are commonly used: the Xe_2*-emission at 172 nm and the Hg-emission at 185 nm. The use of the first is limited in its technical applications by the high absorption cross section of water at 172 nm,[3] but is preferred for mechanistic investigations due to the quasi-monochromatic emission of the radiation source. Xe_2*-lamps have shown a high technical potential for applications in the gas phase.[1,2] At 185 nm, the absorption coefficient of condensed water is more than 200 times lower,[1] yielding therefore a much better prospect of large scale technical applications in the domain of water treatment. Radiation of 185 nm is also absorbed by molecular oxygen, and this line of emission may be used for the treatment of waste gas too. The Hg-emission at 185 nm is combined with that at 254 nm of a low-pressure Hg arc with a synthetic quartz envelope (*e.g.*, Suprasil®). This arc is frequently used for the disinfection of drinking water, for the production of ultra-pure water and for the treatment of waste water as well as waste gases originating from hoods (canteens, chemical and biological laboratories), offices and hospital rooms. Its VUV-emission might reach approx. 10% of the radiative power of the emitted 254 nm line,[4] and the enhancing effect on all kinds of oxidative degradation processes as well as on the biocidal action of the arc was shown.[1] However, only very few quantitative studies have been made so far.

Within the domain of environmental techniques, the 254 nm line is primarily used for the disinfection of drinking water and in UV/H_2O_2-processes for the treatment of waste water. The oxidative degradation of organic compounds (RH) in aqueous systems is initiated by the photolysis of added H_2O_2,[5] the resulting hydroxyl radicals ($HO^{\cdot}$, reaction (1)) attacking the organic compounds by hydrogen abstraction (reaction (2)), electrophilic addition to π-bonds or electron transfer. VUV-radiation implies a double action, as it photolyzes both H_2O (reaction (3)) and H_2O_2 (reaction (1)). In addition, very early publications in this field reported that H_2O_2 was produced during VUV-photolysis of aqueous systems.[6] The observations were taken-up by Azrague *et al*. with a first mechanistic investigation on the fate of the primary radicals ($H^{\cdot}$ and $HO^{\cdot}$) generated in reaction (3) in the presence of dissolved molecular oxygen (O_2).[7] In fact, aiming at a differentiation between and a quantification of the contributions of VUV- and UVC-radiation to the process of photochemically initiated oxidative degradation, the scheme of reactions initiated by the first must be known in detail.

$$H_2O_2 + h\nu\ (\leq 254\ \text{nm}) \rightleftarrows 2HO^{\cdot} \quad (1)$$

$$HO^{\cdot} + RH \rightarrow H_2O + R^{\cdot} \quad (2)$$

[a]*Lehrstuhl für Umweltmesstechnik, Engler-Bunte-Institut, Universität Karlsruhe, D-76131 Karlsruhe, Germany. E-mail: andre.braun@mac.com, andre.braun@kit.edu*
[b]*Heinrich Sontheimer Laboratory of Water Technology, D-76139 Karlsruhe, Germany*

† This article is published as part of a themed issue in honour of Professor Kurt Schaffner on the occasion of his 80th birthday.

‡ Present address: Karlsruher Institut für Technologie (KIT), Campus Süd, Insitut für Technische Thermodynamik und Kältetechnik, 76131 Karlsruhe, Germany
§ Present address: Karlsruher Institut für Technologie (KIT), Campus Süd, Institut für Bio- und Lebensmitteltechnik, Bereich IV: Molekulare Aufarbeitung von Bioprodukten, Engler-Bunte-Ring 1, 76131 Karlsruhe, Germany.
¶ Present address: Karlsruher Institut für Technologie (KIT), Campus Süd, Engler-Bunte-Institut, Engler-Bunte-Ring 1, 76131 Karlsruhe, Germany.

$$H_2O + h\nu\ (< 190\ \text{nm}) \rightleftarrows H^{\cdot} + HO^{\cdot} \quad (3)$$

In a first phase of this work, it was decided to review the few investigations that had been published during the last 8 years. Gonzalez *et al*. repeated in their review of 2005 their earlier hypothesis that the production of H_2O_2 by VUV-photolysis of pure water was taking place mainly by recombination of $HO^{\cdot}$ (reaction (4)).[8] In fact, their hypothesis was supported by the findings of Azrague *et al*. reporting the production of H_2O_2 in nitrogen- (N_2-) saturated H_2O.[7] However, Oppenländer excluded the production of H_2O_2 by reaction (4) on the basis of the rate constants of the competing reactions of the primary radicals (reactions (4)–(6)) generated by reaction (3).[1]

$$HO^{\cdot} + HO^{\cdot} \rightarrow H_2O_2 \quad k_4 = 4 \times 10^9\ M^{-1}\ s^{-1} \quad (4)$$

$$H^{\cdot} + HO^{\cdot} \rightarrow H_2O \quad k_5 = 1.5 \times 10^{10}\ M^{-1}\ s^{-1} \quad (5)$$

$$H^{\cdot} + H^{\cdot} \rightarrow H_2 \quad k_6 = 1 \times 10^{10}\ M^{-1}\ s^{-1} \quad (6)$$

In the presence of O_2, H_2O_2 was found by all authors cited. They explained the significant production of H_2O_2 with an efficient trapping of atomic hydrogen ($H^{\cdot}$) by O_2 (reaction (7)) and, upon deprotonation (equilibrium (8)), with the subsequent oxidation of superoxide ($O_2^{-\cdot}$) by the hydroperoxyl radical ($HO_2^{\cdot}$, reaction (9)) or with the disproportionation of either of the two species (reactions (10) and (11)). However, reactions (12) and (13) were invoked to question the importance of the peroxyl species ($HO_2^{\cdot}$ and $O_2^{-\cdot}$) in the production of H_2O_2. Nevertheless, the production of H_2O_2 in N_2-saturated H_2O by 172 nm-irradiation would finally depend on purging conditions and irradiation time, as O_2 would be produced during the course of the photolysis.

$$H^{\cdot} + O_2 \rightarrow HO_2^{\cdot} \quad k_7 = 2 \times 10^{10}\ M^{-1}\ s^{-1} \quad (7)$$

$$HO_2^{\cdot} + H_2O \rightleftarrows O_2^{-\cdot} + H_3O^+ \quad pK_a = 4.8 \quad (8)$$

$$HO_2^{\cdot} + O_2^{-\cdot} \rightarrow O_2 + HO_2^- \quad k_9 = 5 \times 10^7\ M^{-1}\ s^{-1} \quad (9)$$

$$2HO_2^{\cdot} \rightarrow O_2 + H_2O_2 \quad k_{10} = 1.05 \times 10^6\ M^{-1}\ s^{-1} \quad (10)$$

$$2O_2^{-\cdot} + 2H_2O \rightarrow O_2 + 2HO^- + H_2O_2 \quad k_{11} = 0.3\ M^{-1}\ s^{-1} \quad (11)$$

$$HO_2^{\cdot} + HO^{\cdot} \rightarrow O_2 + H_2O \quad k_{12} = 1.5 \times 10^{10}\ M^{-1}\ s^{-1} \quad (12)$$

$$O_2^{-\cdot} + HO^{\cdot} \rightarrow O_2 + HO^- \quad k_{13} = 1 \times 10^{10}\ M^{-1}\ s^{-1} \quad (13)$$

$$HO^{\cdot} + H_2O_2 \rightarrow H_2O + HO_2^{\cdot} \quad k_{14} = 3.3 \times 10^7\ M^{-1}\ s^{-1} \quad (14)$$

During the VUV-photolysis (172 nm) of air- or O_2-saturated H_2O, the concentration of H_2O_2 reaches a steady state.[6a,7] In fact, H_2O_2 reacts with both primary radicals, but since $H^{\cdot}$ is efficiently trapped by dissolved O_2, the reaction with $HO^{\cdot}$ (reaction (14)) is more important. Calculated relative absorbance spectra of H_2O_2 and H_2O (at the steady state concentration of the first[12]) show that the fraction of radiation absorbed by H_2O_2 at 172 nm and its photolysis (reaction (1)) may be neglected. Nevertheless, as the emission spectra of most Xe_2*-radiation sources are tailing toward 190 nm, photolysis might not be completely excluded at $\lambda_{exc} > 180$ nm.

Azrague *et al.* were apparently the first to investigate on the enhanced production of H_2O_2 during the VUV-photolysis of H_2O in the presence of dissolved organic carbon (DOC).[7] They chose oxalic acid (HOOCCOOH) as a model compound that is mineralized without formation of intermediate compounds. Oxalic acid reacts with $HO^{\cdot}$ by hydrogen abstraction to yield the corresponding oxalyl radical ($HOOCCOO^{\cdot}$, reaction (15)) that eliminates subsequently CO_2 to form the formyl radical ($^{\cdot}COOH$, reaction (16)). As the reaction system was getting more alkaline, hydrogen abstraction of oxalate ($HOOCCOO^-$) was also taken into account (reaction (17)) to yield an oxalyl radical anion that would subsequently fragment into CO_2 and the carbonyl radical anion ($CO_2^{-\cdot}$, reaction (18)). Both, $^{\cdot}COOH$ and $CO_2^{-\cdot}$ react with O_2 to yield the H_2O_2-precursors $HO_2^{\cdot}$ and $O_2^{-\cdot}$ (reactions (19) and (20)).[13]

$$HOOCCOOH + HO^{\cdot} \rightarrow HOOCCOO^{\cdot} + H_2O \quad k_{15} = 7.7 \times 10^6\ M^{-1}\ s^{-1}[14] \quad (15)$$

$$HOOCCOO^{\cdot} \rightarrow CO_2 + {}^{\cdot}COOH \quad (16)$$

$$HOOCCOO^- + HO^{\cdot} \rightarrow {}^-OOCCOO^{\cdot} + H_2O \quad (17)$$

$${}^-OOCCOO^{\cdot} \rightarrow CO_2 + CO_2^{-\cdot} \quad (18)$$

$${}^{\cdot}COOH + O_2 \rightarrow CO_2 + HO_2^{\cdot} \quad (19)$$

$${}^{\cdot}COO^- + O_2 \rightarrow CO_2 + O_2^{-\cdot} \quad (20)$$

The results reported by Azrague *et al*. show a fast increase of $[H_2O_2]$, until a maximum was reached ($[H_2O_2]_{max}$) at approx. 25% of substrate conversion. $[H_2O_2]_{max}$ corresponded to approx. 4 times the stationary $[H_2O_2]$ ($[H_2O_2]_{ss}$) in pure O_2-saturated water. With diminishing substrate concentration, $[H_2O_2]$ was decreasing until $[H_2O_2]_{ss}$ was reached.[7]

Imoberdorf *et al*. chose formic acid (HCOOH) and/or formate ($HCOO^-$) as model compounds that upon hydrogen abstraction by $HO^{\cdot}$ yields $^{\cdot}COOH$ and/or its deprotonated form (reactions (21) and (22)).[15] They used, however, a VUV-emitting Hg low-pressure arc. Nevertheless, the experimental results exhibited an increase of $[H_2O_2]$ until approx. 75% conversion of the organic substrate, and model calculations yielded $[H_2O_2]_{max}$ at irradiation times, when complete mineralization was reached.

$$HCOOH + HO^{\cdot} \rightarrow {}^{\cdot}COOH + H_2O\ 1 \times 10^8\ M^{-1}\ s^{-1} \quad (21)$$

$$HCOO^- + HO^{\cdot} \rightarrow {}^{\cdot}COO^- + H_2O \quad (22)$$

In this work, aqueous methanol (CH_3OH) was chosen as a model system. CH_3OH may be homolyzed by VUV photolysis at 172 nm, but $[CH_3OH]$ may be kept low and its absorbance at 172 nm negligible when compared to that of H_2O.[13] Subsequent to reactions (3) and (23), the scheme of reactions leading to the

mineralization of CH_3OH[8,13] includes primarily reactions (24) to (31).

$$CH_3OH + HO^{\cdot} \rightarrow {}^{\cdot}CH_2OH + H_2O \quad 1 \times 10^9\ M^{-1}\ s^{-1}{}^{8} \quad (23)$$

$${}^{\cdot}CH_2OH + O_2 \rightarrow {}^{\cdot}O_2CH_2OH \quad (24)$$

$${}^{\cdot}O_2CH_2OH \rightarrow CH_2O + HO_2^{\cdot} \quad (25)$$

$$CH_2O + H_2O \rightleftarrows CH_2(OH)_2 \quad (26)$$

$$2\,{}^{\cdot}O_2CH_2OH \rightarrow HOCH_2OOOOCH_2OH \quad (27)$$

$$HOCH_2OOOOCH_2OH \rightarrow 2HCOOH + H_2O_2 \quad (28)$$

$$CH_2(OH)_2 + HO^{\cdot} \rightarrow {}^{\cdot}CH(OH)_2 + H_2O \quad 1 \times 10^9\ M^{-1}\ s^{-1}{}^{8} \quad (29)$$

$${}^{\cdot}CH(OH)_2 + O_2 \rightarrow {}^{\cdot}O_2CH(OH)_2 \quad (30)$$

$${}^{\cdot}O_2CH(OH)_2 \rightarrow HCOOH + HO_2^{\cdot} \quad (31)$$

and, subsequently, reactions (21) and (19).

CH_3OH does not absorb in the UVC spectral domain, does not interact with most of inorganic and organic compounds that might be present in aqueous reaction systems and exists in only one form. As with oxalic and formic acid, the mechanism of its oxidative degradation is known in detail.[8,13] This investigation concentrates on the use of a Xe_2*-radiation source and therefore on a quasi-monochromatic irradiation at 172 nm. It focuses on the primary parameters governing the production of H_2O_2. The results will provide the basis for a differentiation of the respective contributions of VUV- and UVC-initiated photolyses of H_2O and H_2O_2 to the overall result of oxidative degradation of organic compounds dissolved in aqueous media.

Experimental

Irradiation equipment

Irradiation experiments were carried out in an annular reactor (volume: 0.24 L) of negative irradiation geometry equipped with a self-built Xe_2*-radiation source (electric power: 100 W) emitting at 172 nm. The radiant power was determined by methanol actinometry[13] to be 6 W ± 0.7 W. The reactor was mounted into a semi-batch system, in which the aqueous reaction system was circulated between a reservoir and the photochemical reactor (Fig. 1).

Photolyses

For all photochemical experiments, a total volume of 3.7 L of pure water or aqueous methanol solution was used, the water being prepared by ion exchange and reverse osmosis. Methanol (Roth, HPLC grade >99.9%) was used at concentrations from 0.25 to 1.00 mM. The reaction system was gas saturated for 20 min before and for the duration of the experiment by gentle purging of the volume present in the reservoir. Continuous purging with oxygen or nitrogen was needed to avoid oxygen depletion or the presence of oxygen, depending on the experiment. O_2 and N_2 were purchased at highest purity from Air Liquide. Continuous purging was thought to lead to a loss of methanol. In fact, corresponding analyses revealed a loss of < 2% of the amount added.

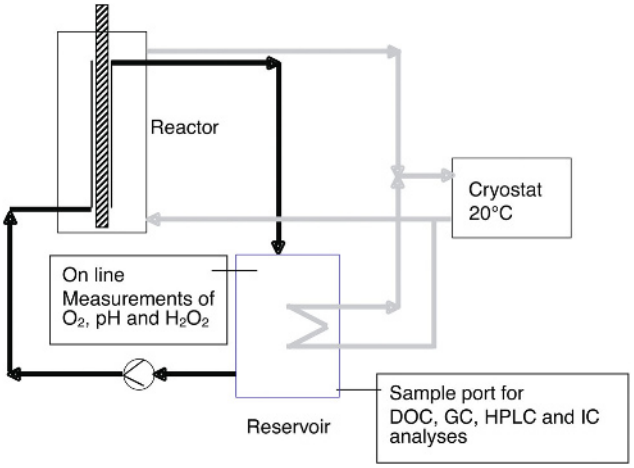

Fig. 1 Scheme of the experimental setup.

The flux of the reaction system was chosen to be 4.8 L min^{-1} (Schmitt, Kreiselpumpe Typ MPN 80, PVDF; Rotameter: Krohne G19.08). Thermoregulation was effected by a cooling liquid circulating between the cryostat (Julabo 10-C 1130W), the reservoir and the reactor and kept at 20 °C. Samples (20 mL) were taken periodically during the experiments.

During all experiments, the concentrations of molecular oxygen ($[O_2]$) and hydrogen peroxide ($[H_2O_2]$) as well as the pH-value of the reaction system were measured on line.

Analyses

DOC analyses were made with a Shimadzu, TOC 5000A with a sensitivity of 0.4 ppm using a high sensitivity catalyst.

On line O_2 analyses were made in the reservoir with a WTW Oximeter OXI 96.

On line pH measurements were made in the reservoir with a WTW pH 340i.

On line H_2O_2 analyses were made in the reservoir by means of fluorescence measurements using an Degussa Aerolaser AL2002.[16] This method of analysis is based on the reaction of H_2O_2 with 4-hydroxyphenyl acetic acid, catalysed by peroxidase. The fluorescence of the resulting 6,6′-dihydroxybiphenyl-3,3′-diacetic acid is measured at a wavelength between 400 to 420 nm. The limit of error was estimated to be ±5%.

Analyses of organic compounds

Methanol and its oxidation products were analyzed as already described.[13] The concentrations of methanol ($[CH_3OH]$) and of ethylene glycol ($[(CH_2OH)_2]$) were determined by gas chromatography using a HP6890, column: HP-Innowax 30 m, diameter: 320 μm. Water contained in the samples was eliminated by a pre-column (empty capillary, length: 5 m). Mobile phase: He, constant flow: 2.6 mL min^{-1}; FID.

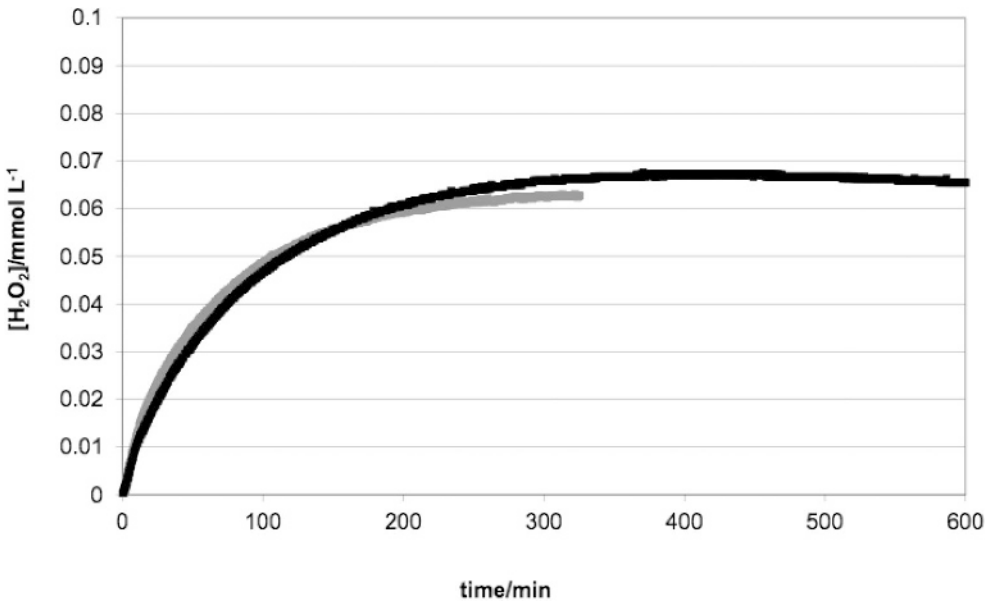

Fig. 2 VUV-photolysis (172 nm) of air-saturated pure water. Evolution of $[H_2O_2]$ with irradiation time. Examples of two independent experiments to confirm the reproducibility of the procedures.

The concentrations of formic ([HCOOH]) and of oxalic ($[(COOH)_2]$) acid were determined by ion chromatography with a Dionex DX 500, equipped with an anion separation column AS14 (250 × 4 mm) and a pre-column AG14 (50 × 4 mm), carrier material: polystyrene/divinyl benzene resin particles, 9 μm. Eluent: 3.5 mM $NaHCO_3^{-1}$ mM Na_2CO_3, flux: 1.2 L min^{-1}; conductivity detector.

After derivatization with 2,4-dinitrophenyl hydrazine, the concentration of formaldehyde ($[CH_2O]$) was determined by HPLC using a HP1100, column: LiChrospher 100 RP-18 (4 × 125 mm) on polar modified silica gel, 5 μm. Eluent: 60% Na–acetate buffer, 40% acetonitrile), flux: 1 mL min^{-1}.

Catalase (100 μL/20 mL of sample) was added to all samples in order to eliminate H_2O_2, hence, preventing reactions after sampling. The limit of error was estimated to be ±3%.

Results and discussion

The experimental work was divided into two parts. The first concerned the effect of CH_3OH on the production of H_2O_2, and therefore series of experiments were made with different initial concentrations ($[CH_3OH]_0$) ranging from 0 to 1 mM. In a second part, the effect of the concentration of dissolved molecular oxygen ($[O_2]$) on the production of H_2O_2 and on the reaction products of the oxidation of CH_3OH was investigated. Blank (reference) experiments (absence of CH_3OH: see Fig. 2, and with 0.25 mM CH_3OH: see Fig. 3) were repeatedly performed to ensure reproducibility. The differences between the curves shown in Fig. 2 and 3, respectively, are within the range of error of the H_2O_2-analyzer.

As expected, the evolution of $[H_2O_2]$ with irradiation time depended strongly on $[CH_3OH]_0$ (Fig. 4). The corresponding maxima ($[H_2O_2]_{max}$) and the time at which these maxima were reached were getting larger with increasing $[CH_3OH]_0$.

In order to understand this result, at least qualitatively, the rather complex reaction system [*e.g.* ref. 15] was restricted to those reactions affecting primarily production and consumption of H_2O_2. Among the reactions involving the primary radicals $H^{\cdot}$ and $HO^{\cdot}$, reactions (4)–(6), and among the reactions involving the precursors of H_2O_2 production, reactions (10)–(13), were neglected in eqn (32). The observation that H_2O_2 is not produced in the absence of O_2 is indicating that reaction (4) has not to be taken into account. The rate of in-cage recombination (5) is very high and may be assumed constant and independent of the parameter variations made in this work. Reaction (5) is therefore only affecting the efficiency (apparent quantum yield) of the production of the primary radicals. Out of cage reaction (6) is disfavoured against in-cage reaction (5) and against reaction (7) due to the relative high concentrations of dissolved O_2 in use. Reactions (10) and (11) are not competitive under the chosen experimental conditions (pH). Under conditions of $[O_2]$ = const. and $[CH_3OH]_0$ = 0 mM, it may be therefore assumed that H_2O_2 is produced most efficiently by reaction (9) and consumed fastest in reaction (14).

$$\frac{\delta[H_2O_2]}{\delta t} = k_9[HO_2^{\cdot}][O_2^{-\cdot}] - k_{14}[H_2O_2][HO^{\cdot}] \qquad (32)$$

In the absence of CH_3OH, an increase of $[H_2O_2]$ was observed, until a steady-state concentration ($[H_2O_2]_{ss}$) was reached. $[H_2O_2]_{ss}$ represents conditions where rates of production and consumption are equal.

$$\frac{\delta[H_2O_2]}{\delta t} = k_9[HO_2^{\cdot}][O_2^{-\cdot}] - k_{14}[H_2O_2]_{ss}[HO^{\cdot}] = 0 \qquad (33)$$

hence

$$[H_2O_2]_{ss} = \frac{k_9[HO_2^{\cdot}][O_2^{-\cdot}]}{k_{14}[HO^{\cdot}]} \qquad (34)$$

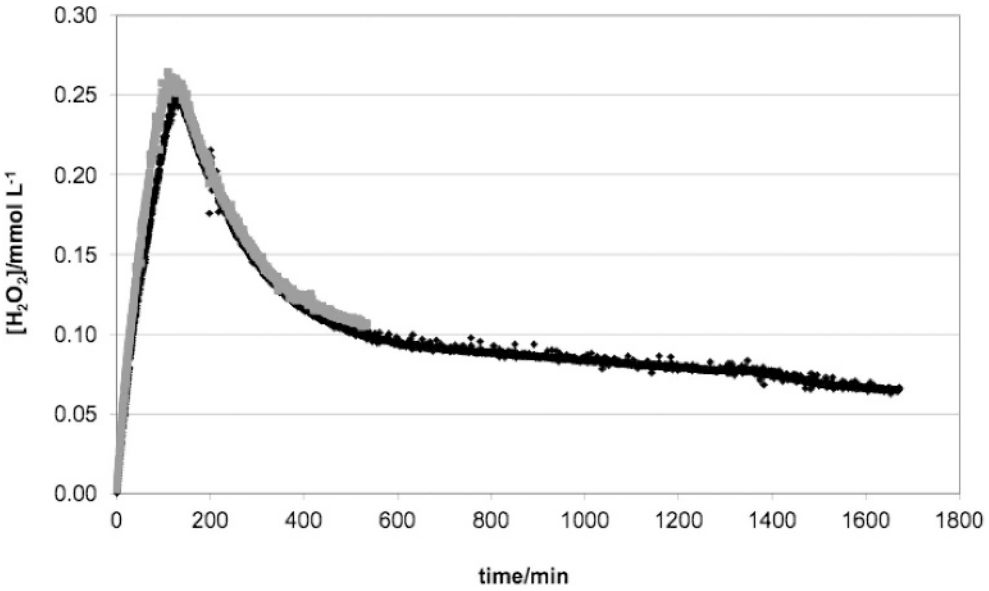

Fig. 3 VUV-photolysis (172 nm) of air-saturated 0.25 mM aqueous CH_3OH. Evolution of $[H_2O_2]$ with irradiation time. Examples of two independent experiments to confirm the reproducibility of the procedures.

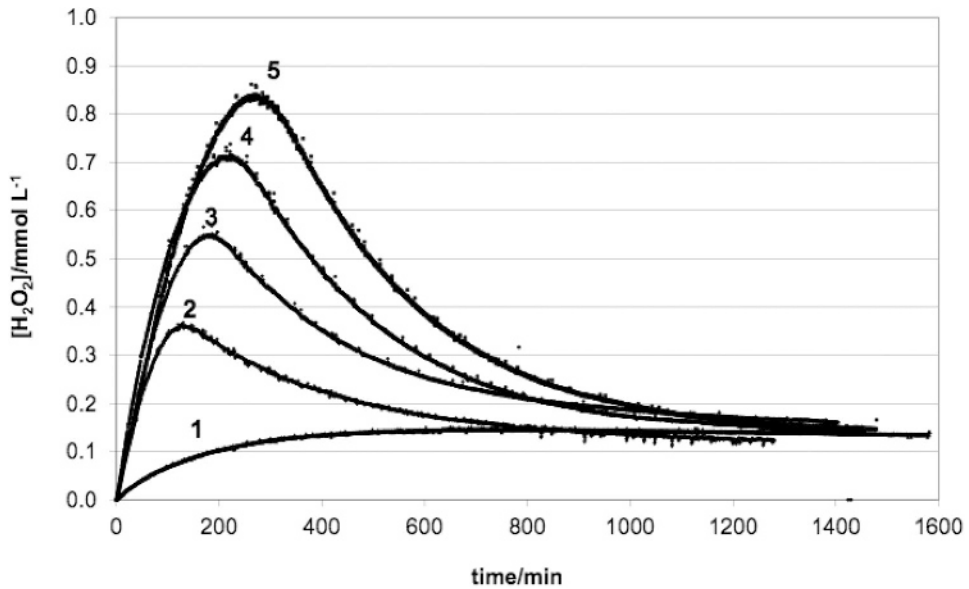

Fig. 4 Evolution of $[H_2O_2]$ produced by VUV-photolysis (172 nm) of O_2-saturated aqueous CH_3OH of varying initial concentrations. $[CH_3OH]_0$: (**1**) 0 mM; (**2**) 0.25 mM; (**3**) 0.50 mM; (**4**) 0.75 mM; (**5**) 1.00 mM.

Eqn (35) shows the dependence of $[HO^{\cdot}]$ at a given time t on the photochemical parameters.

$$\frac{\delta[HO^{\cdot}]}{\delta t} = P_a\Phi_{HO^{\cdot}} - k_{12}\frac{[O_2^{-\cdot}][H^+]}{K_A}[HO^{\cdot}] - k_{13}[O_2^{-\cdot}][HO^{\cdot}] - k_{14}[H_2O_2][HO^{\cdot}] = 0 \quad (35)$$

where P_a: absorbed photon flux [einstein s^{-1}], $\Phi_{HO^{\cdot}}$: apparent quantum yield of $HO^{\cdot}$ generation by VUV photolysis of H_2O.

Under conditions, where $[H_2O_2]$ varies with time, either the rate of production or the rate of consumption is faster. For $[CH_3OH]_0 > 0$ mM, fast increases of $[H_2O_2]$ were registered (Fig. 4), until maximum concentrations ($[H_2O_2]_{max}$) were reached that depended on $[CH_3OH]_0$. Subsequently, $[H_2O_2]$ diminished to level off to $[H_2O_2]_{ss}$.

In the presence of CH_3OH, eqn (35) is extended for reaction (23).

$$\frac{\delta[HO^{\cdot}]}{\delta t} = P_a\Phi_{HO^{\cdot}} - k_{12}\frac{[O_2^{-\cdot}][H^+]}{K_A}[HO^{\cdot}] - k_{13}[O_2^{-\cdot}][HO^{\cdot}] - k_{14}[H_2O_2][HO^{\cdot}] - k_{23}[CH_3OH][HO^{\cdot}] = 0 \quad (36)$$

The kinetics of the oxidative degradation of 1 mM aqueous CH_3OH is visualized in Fig. 5. The sequence of reactions

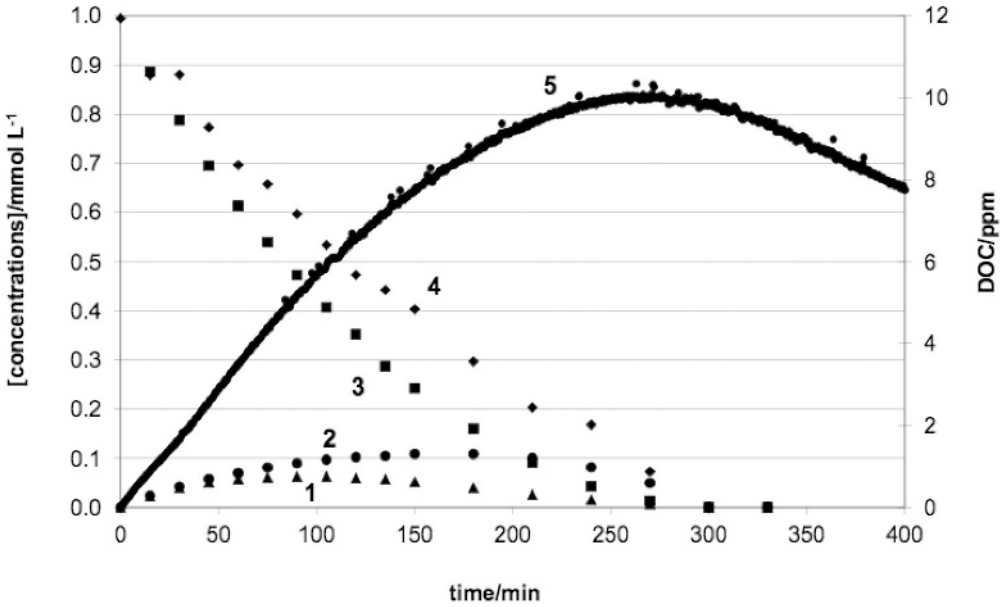

Fig. 5 VUV-photolysis of O_2-saturated 1.0 mM aqueous CH_3OH. Evolution of [HCOOH] (**1**), [CH_2O] (**2**), [CH_3OH] (**3**), DOC (**4**) and [H_2O_2] (**5**) with time of irradiation.

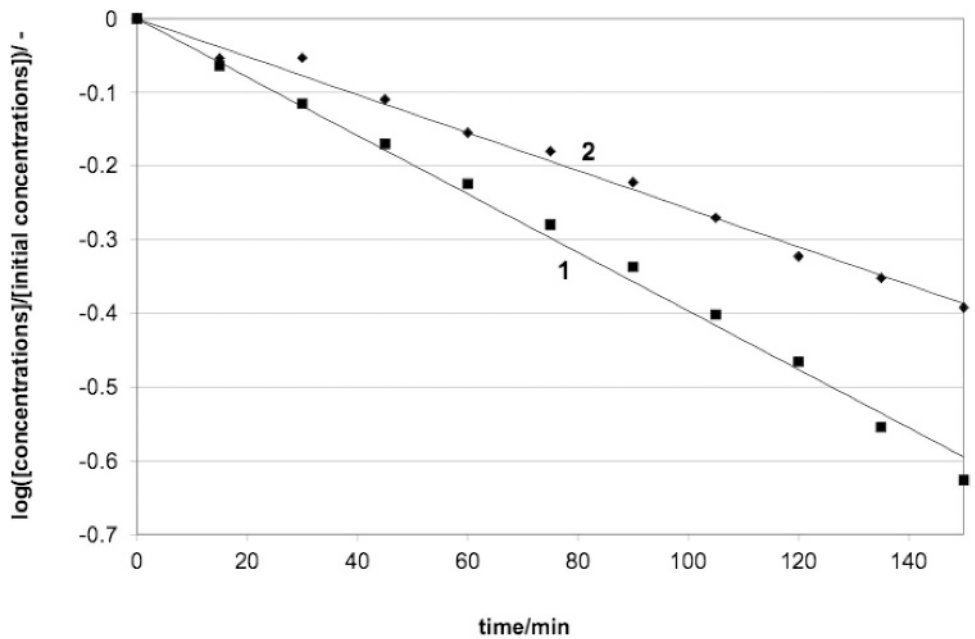

Fig. 6 VUV-photolysis of O_2-saturated 1.0 mM aqueous CH_3OH. Kinetics of [CH_3OH] (**1**) and DOC (**2**) diminution.

leading to the mineralization of CH_3OH (reactions (23) to (31) and reactions (21) and (19)) passes *via* formaldehyde (CH_2O) and formic acid (HCOOH) that react with $HO^{\cdot}$ (reactions (29) and (21), respectively) and therefore affect the evolution of [H_2O_2].

The evolution of [CH_3OH] with time of irradiation followed pseudo-first order kinetics up to approx. 60% of conversion (Fig. 6). $[H_2O_2]_{max}$ was reached at ≥95% of conversion of CH_3OH, but still in the presence of approx. 20% of DOC_0.

These results imply that reactions (21) and (29) should also be part of eqn (36). In accord with the scheme of reactions introduced for the mineralization of CH_3OH, 3 $HO^{\cdot}$ are needed to initiate oxidation of the substrate and the two intermediate compounds. Assuming that the rate constants of these three reactions (23), (28) and (21) are within the same order of magnitude, eqn (36) must be corrected accordingly.

$$\frac{\delta[HO^{\cdot}]}{\delta t} = P_a\Phi_{HO^{\cdot}} - k_{12}\frac{[O_2^{-\cdot}][H^+]}{K_A}[HO^{\cdot}] - k_{13}[O_2^{-\cdot}][HO^{\cdot}] - k_{14}[H_2O_2][HO^{\cdot}] - k_{23}3[CH_3OH][HO^{\cdot}] = 0 \quad (37)$$

The adopted mechanistic hypothesis does not include a reaction between CH_3OH and H_2O_2, and there is experimental evidence that, under the experimental conditions chosen, the rate of such a reaction is too slow to be taken into account.

Consequently, the impact of added CH_3OH on the evolution of $[H_2O_2]$. may be evaluated by substituting $[HO^{\cdot}]$ (eqn (37)) in eqn (32).

$$\frac{\delta[H_2O_2]}{\delta t} = k_9 \frac{[O_2^{-\cdot}][H^+]}{K_A}[O_2^{-\cdot}] - k_{14}[H_2O_2] \times \frac{P_a\Phi_{HO^{\cdot}}}{k_{12}\frac{[O_2^{-\cdot}][H^+]}{K_A} + k_{13}[O_2^{-\cdot}] + k_{14}[H_2O_2] + k_{23}3[CH_3OH]_0} \quad (38)$$

Addition of CH_3OH provokes a rather steep increase of $[H_2O_2]$ ($(\delta[H_2O_2]/\delta t) > 0$) upon VUV-irradiation of the aqueous reaction system, until a maximum is reached ($(\delta[H_2O_2]_{max}/\delta t) = 0$). Eqn (38) was resolved to obtain $[H_2O_2]_{max}$.

$$[H_2O_2]_{max} = \frac{k_9\frac{[O_2^{-\cdot}][H^+]}{K_A}[O_2^{-\cdot}]\left(k_{12}\frac{[O_2^{-\cdot}][H^+]}{K_A} + k_{13}[O_2^{-\cdot}] + k_{23}3[CH_3OH]_0\right)}{k_{14}\left(P_a\Phi_{HO^{\cdot}} - k_9\frac{[O_2^{-\cdot}][H^+]}{K_A}[O_2^{-\cdot}]\right)} \quad (39)$$

At very high concentrations of $[CH_3OH]_0$ with respect to those of the peroxyl species, the summands $k_{12}(([O_2^{-\cdot}][H^+])/K_A) + k_{13}[O_2^{-\cdot}]$ become negligible, and the asymptotic function $[H_2O_2]_{max} = f([CH_3OH]_0)$ will reach a value controlled by

$$[H_2O_2]_{max} = \frac{k_9\frac{[O_2^{-\cdot}][H^+]}{K_A}[O_2^{-\cdot}]k_{23}3[CH_3OH]_0}{k_{14}\left(P_a\Phi_{HO^{\cdot}} - k_9\frac{[O_2^{-\cdot}][H^+]}{K_A}[O_2^{-\cdot}]\right)} \quad (40)$$

and

$$\frac{1}{[H_2O_2]_{max}} = \frac{k_{14}}{k_{23}3[CH_3OH]_0}\left(\frac{P_a\Phi_{HO^{\cdot}}}{k_9\frac{[O_2^{-\cdot}][H^+]}{K_A}[O_2^{-\cdot}]} - 1\right) \quad (41)$$

In the case of high $[CH_3OH]_0$, $[O_2^{-\cdot}]$ remains very small, but there are no means to determine the respective range of concentrations. In the opposite case, where $[CH_3OH]_0 = 0$ (eqn (42)), $[O_2^{-\cdot}]$ cannot exceed values of approx. 5×10^{-7} mM under the experimental conditions applied, because factor

$$\frac{P_a\Phi_{HO^{\cdot}}}{k_9(([O_2^{-\cdot}][H^+])/K_A)[O_2^{-\cdot}]} - 1$$

in eqn (43) cannot attain values ≤ 0.

$$[H_2O_2]_{max} = \frac{k_9\frac{[O_2^{-\cdot}][H^+]}{K_A}[O_2^{-\cdot}]\left(k_{12}\frac{[O_2^{-\cdot}][H^+]}{K_A} + k_{13}[O_2^{-\cdot}]\right)}{k_{14}\left(P_a\Phi_{HO^{\cdot}} - k_9\frac{[O_2^{-\cdot}][H^+]}{K_A}[O_2^{-\cdot}]\right)} \quad (42)$$

$$\frac{1}{[H_2O_2]_{max}} = \frac{k_{14}}{\left(k_{12}\frac{[O_2^{-\cdot}][H^+]}{K_A} + k_{13}[O_2^{-\cdot}]\right)}\left(\frac{P_a\Phi_{HO^{\cdot}}}{k_9\frac{[O_2^{-\cdot}][H^+]}{K_A}[O_2^{-\cdot}]} - 1\right) \quad (43)$$

Beyond $[H_2O_2]_{max}$, the decreasing $[CH_3OH]$ slows down the rate of reaction (23), and the increasing availability of $HO^{\cdot}$ leads to a diminution of $[H_2O_2]$ ($\delta[H_2O_2]/\delta t < 0$). With the total consumption of DOC (eqn (37): $[CH_3OH] = 0$), stationary conditions ($[H_2O_2]_{ss}$) are resumed.

In order to derive from the experiments reported the impact of added CH_3OH on the production of H_2O_2, means must be developed to determine the additional amount of H_2O_2 produced, with respect to the blank experiment made in the absence CH_3OH. On line $[H_2O_2]$ measurements yield the momentaneously available $[H_2O_2]$ at irradiation times t. Integration of eqn (38) would take into account varying rates of production and consumption of H_2O_2 with changing $[HO^{\cdot}]$ during irradiation time. The authors had no means to undertake such model calculation.

Numerical integration of the experimentally determined $[H_2O_2]$ over an irradiation time long enough to take into account all variations of those rates, and subsequent normalization of these integrated values with respect to that of the blank experiment eliminate concerns about varying rates and accumulation of H_2O_2 and provide quantitative data reflecting the effect of CH_3OH addition. In accord with the results shown in Fig. 4, $[H_2O_2]$-values were integrated from t_0 to t = 1400 min, where the respective $[H_2O_2]$ in all experiments reported might be considered equal ($[H_2O_2]_{ss}$). As shown in Fig. 7, these normalized values depend linearly on $[CH_3OH]_0$. The slope of the curve was determined to be 2.3 mM^{-1}, showing that one mM of CH_3OH added produces more than two mM of additional H_2O_2. The result is rather close to the factor expected on the basis of additional $HO^{\cdot}$ consumed in reactions (21), (23) and (29). Linearity and slope of that dependence might depend on the range on $[CH_3OH]_0$ investigated as well as on P_a due to the heterogeneity of the photochemical reaction system.

In a second phase of this work, the effect of dissolved O_2 was investigated. The production of H_2O_2 by VUV-photolysis of pure water was explained earlier to take place mainly by recombination of $HO^{\cdot}$ (eqn (4)).[6a,7,8] Azrague *et al.* also mention reaction (4) to explain their results obtained with nitrogen saturated H_2O.[7] The results shown in Fig. 8 confirm, however, the conclusions made by Oppenländer[1] as far as the H_2O_2-production in the absence of O_2 is concerned. The respective result of Azrague *et al.*[7] might be due to an equipment failure, as they saturated the reaction system with N_2 prior the photolyses but stopped purging during irradiation. The reported identical evolution of $[H_2O_2]$ in the presence and absence of oxalic acid confirms known kinetic data implying that reaction (7) is far more important for the production of H_2O_2 than reaction sequence (16) to (21).[7,10,14] Their observation of an increase of $[H_2O_2]_{ss}$ with increasing $[O_2]$ is affirmed by the results shown in Fig. 8. $[H_2O_2]_{ss}$ was found to be 0.06 to 0.07 mM in air-saturated ($[O_2]$: 2.5×10^{-1} mM, Fig. 2 and 3) and 0.12 (Fig. 5) to 0.14 mM (Fig. 4 and 8) in O_2-saturated ($[O_2]$: 1.25 mM) H_2O. The results leave no doubt that $[H_2O_2]_{ss}$ depends primarily on the rate of reaction (7), *i.e.* the trapping of $H^{\cdot}$ by O_2. The dependence of $[H_2O_2]_{ss}$ on $[O_2]$ (Fig. 8) indicates an asymptotic behaviour, the final value of $[H_2O_2]_{ss}$ remaining, however, theoretical, as $[O_2]$ cannot be further enhanced under normal pressure conditions.

Fig. 9 exhibits the interdependence of H_2O_2, O_2 and the pH-value of the reaction system containing 0.25 mM CH_3OH. Taking into account the purging procedure and the volume of the aqueous reaction system involved in every experiment, the diminution of $[O_2]$ during the enhanced production of H_2O_2 is

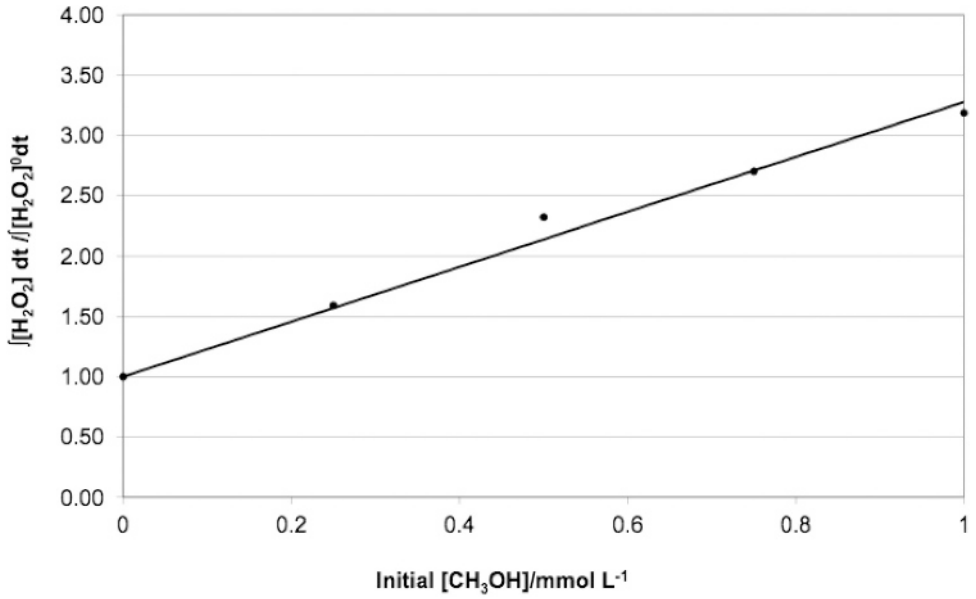

Fig. 7 Linear dependence of the integrated and normalized values ($\int_0^{1400\ min}[H_2O_2]dt/\int_0^{1400\ min}[H_2O_2]^0dt$) produced by VUV photolysis (172 nm) of O_2-saturated aqueous CH_3OH on $[CH_3OH]_0$.

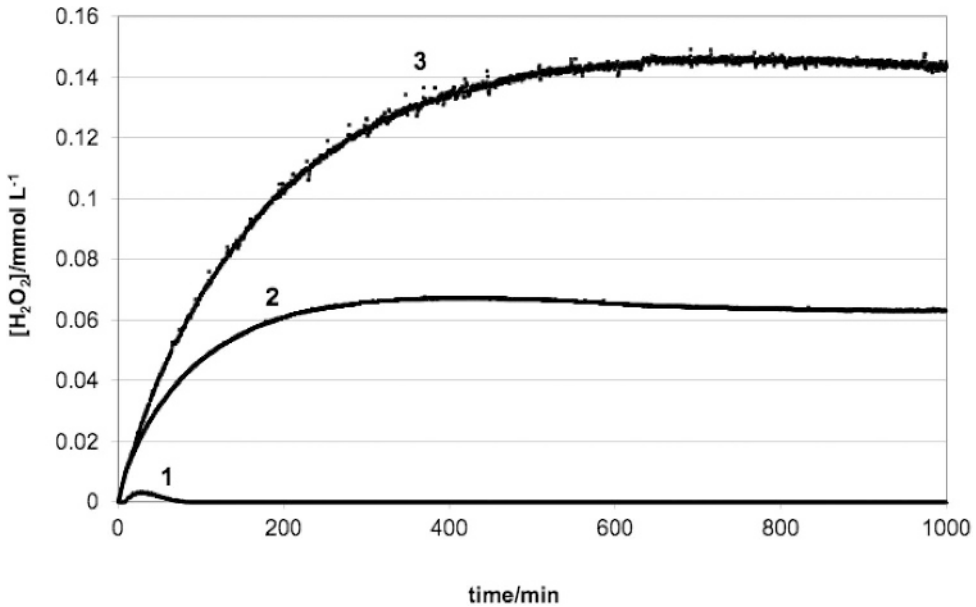

Fig. 8 VUV-photolysis of pure H_2O. Dependence of the evolution of $[H_2O_2]$ on $[O_2]$. (**1**) 0 mM O_2 (N_2-saturation); (**2**) 0.25 mM O_2 (air-saturation); (**3**) 1.25 mM O_2 (O_2-saturation).

surprising. Earlier investigations on the oxidative degradation of phenol in a stirred batch reactor showed that the consumption of the substrate was paralleled by a diminution of $[O_2]$ in function of the distance from the lamps surface and in function of the actual DOC, and followed pseudo-first order kinetics despite the local diminution of $[O_2]$.[3a,13b] Given (i) the (primarily highly localized) O_2 depletion and (ii) the fact that in air-saturated reaction systems, reactions between $H^{\cdot}$ and organic compounds are not competitive when compared to reaction (7), the same may apply during an 80% $[O_2]$ depletion, as shown in Fig. 9. Depending on lifetimes, $H^{\cdot}$ and C-centered radicals will be trapped by O_2 at rather short distances from the lamp, whereas radicals originating from the thermal decomposition of (hydro) peroxides will react with O_2 in the bulk of the reaction system. The pH-value of the reaction system remained stable indicating that the subsequent appearance of carboxylic and carbonic acid is compensated by the production of HO^- in subsequent thermal reactions. In accordance with the results shown in Fig. 4, steady-state experimental conditions would be reached after approx. 1400 min. At that time, $[H_2O_2]$ should have dropped to 0.06 mM (see Fig. 2 and 3), and $[O_2]$-measurements should indicate air-saturation (0.25 mM).

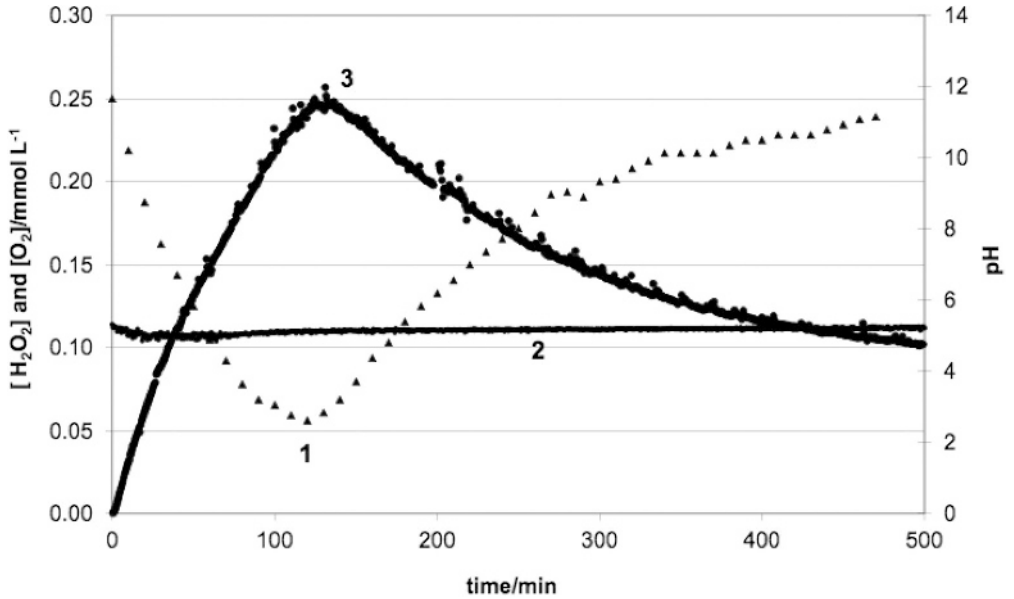

Fig. 9 VUV-photolysis of air-saturated H_2O containing 0.25 mM of CH_3OH. Evolution of $[O_2]$ (**1**), pH-value (**2**) and $[H_2O_2]$ (**3**).

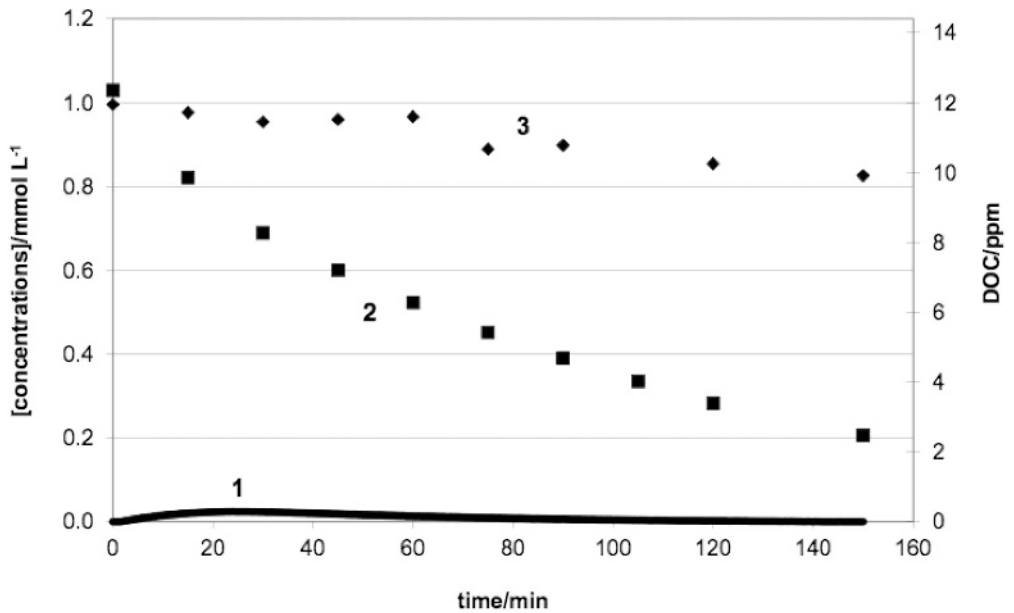

Fig. 10 VUV-photolysis of N_2-saturated 1.0 mM aqueous CH_3OH. Evolution of $[H_2O_2]$ (**1**), $[CH_3OH]$ (**2**) and DOC (**3**) with time of irradiation.

The results of the VUV-photolysis of N_2-saturated 1.0 mM aqueous CH_3OH are reported in Fig. 10. As already explained earlier, the diminution of $[CH_3OH]$ and DOC is mainly due to $HO^{\cdot}$-initiated oxidation (H-abstractions and electron transfer), and an additional enhancement of the oxidative degradation (*e.g.* H-abstraction by organic peroxyl radicals) may be neglected. In addition, these experimental conditions were shown to favour reductions by $H^{\cdot}$ and C-centred radicals[17] leading to the (re)production of substrate and different organic compounds without loss of DOC. Disproportionation (reaction (44)) and recombination (reaction (45)) of $^{\cdot}CH_2OH$ were described earlier.[8,13,18]

$$2\,^{\cdot}CH_2OH \rightarrow CH_3OH + CH_2O \quad (44)$$

$$2\,^{\cdot}CH_2OH \rightarrow OHCH_2CH_2OH \quad (45)$$

Experiments with N_2-saturated aqueous solutions of 1.0 mM of CH_3OH (Fig. 10) confirm the result reported for N_2-saturated H_2O (see also Fig. 8). O_2 definitely mediates the production of H_2O_2 *via* reactions (7), (20), (24) and (30). The very small signal of H_2O_2 shown in Fig. 10 might be due to traces of O_2 or electrical distortions.

Conclusion

The production of H_2O_2 during VUV-photolysis of aqueous reaction systems was observed very early, in particular, after Xe_2*-radiation sources were introduced to the domains of preparative photochemistry and photochemical environmental techniques. Previous investigations by a few research groups yielded first quantitative analytical results that refined the scheme of reactions subsequent to the photochemical homolysis of H_2O. The results presented in this paper focus exclusively on the VUV-photolysis of H_2O and confirm (1) the production of H_2O_2 in the presence of O_2 and (2) the enhanced production of H_2O_2 in aqueous solutions of organic compounds, using CH_3OH as a model compound.

No H_2O_2 could be found in the absence of O_2, therefore the recombination of $HO^{\cdot}$ radicals (reaction (4)) might be neglected. However, in the presence of O_2, $H^{\cdot}$ is trapped by O_2 yielding $HO_2^{\cdot}$ (reaction (7)), which is instrumental for the production of H_2O_2 (reactions (9) to (11)). H_2O_2, $HO_2^{\cdot}$ and $O_2^{-\cdot}$ react with $HO^{\cdot}$ (reactions (12) to (14)), and in the absence of DOC, steady state conditions are established. $[H_2O_2]_{ss}$ depends mainly on $[O_2]$, *i.e.* on the efficiency of $H^{\cdot}$ trapping.

The enhanced production of H_2O_2 in aqueous solutions of organic compounds may be primarily assigned to reactions of $HO^{\cdot}$ with the model compound investigated (CH_3OH) as well as with all the intermediate compounds produced in the course of oxidative degradation (mineralization). Consequently, the rates of the $HO^{\cdot}$ reactions with H_2O_2 and the inorganic peroxyl species diminish, and higher $[H_2O_2]$ remain in the reaction system.

The results show that the evolution of $[O_2]$ is linked with that of the enhanced production of H_2O_2, as the amounts of $HO^{\cdot}$ (reacting with DOC) and of O_2 (reacting with the C-centred radicals) are comparable. Expectedly, an almost oxidation equivalent relation was found between H_2O_2, additionally produced in the presence of organic compounds, and the corresponding $[CH_3OH]_0$.

Kinetic studies resulted in equations for steady-state conditions in the absence and in the presence of DOC ($[H_2O_2]_{ss}$ and $[H_2O_2]_{max}$, respectively). The asymptotic behaviour of $[H_2O_2]_{max}$ in function of $[CH_3OH]_0$ (Fig. 4) could be confirmed on the basis of kinetic equations. The combined results will be most helpful to assess H_2O_2 production and consumption in, and the respective contributions of VUV- and UVC-initiated photolyses of H_2O and H_2O_2 to the overall result of oxidative degradation of organic compounds dissolved in aqueous media.

References

1 T. Oppenländer, *Photochemical Purification of Water and Air: Advanced Oxidation Processes (AOPs): Principles, Reaction Mechanisms, Reactor Concepts*, Wiley-VCH, Weinheim, 2003, ISBN: 978-3-527-30563-6, pp. 200–213.

2 (*a*) C. Baus, K. Schaber, I. Gassiot Pintori and A. M. Braun, *Sep. Purif. Technol.*, 2002, **28**, 125–140; (*b*) I. Gassiot Pintori, *Untersuchungen VUV-photochemisch induzierter Prozesse zum Abbau von Schadstoffen in der Gasphase*, Dissertation, Fakultät für Chemieingenieurwesen und Verfahrenstechnik, Universität Karlsruhe (TH), Karlsruhe, 2001.

3 (*a*) G. Heit and A. M. Braun, *J. Inf. Rec.*, 1996, **22**, 543–546; (*b*) G. Heit and A. M. Braun, *Water Sci. Technol.*, 1997, **35**, 25–30.

4 T. M. Hashem, *The Use of VUV and UV-C Light Sources for Advanced Oxidation Processes*, Dissertation, Fakultät für Chemieingenieurwesen und Verfahrenstechnik, Universität Karlsruhe (TH), Karlsruhe, 1998.

5 O. Legrini, E. Oliveros and A. M. Braun, *Chem. Rev.*, 1993, **93**, 671–698.

6 (*a*) T. Aminian-Saghafi, *Reactivité du peroxide d'hydrogène dans des microemulsions*, Thèse Nr. 873, Ecole Polytechnique Fédérale de Lausanne, Lausanne, 1990; (*b*) L. Jakob, T. M. Hashem, S. Bürki, N. M. Guindy and A. M. Braun, *J. Photochem. Photobiol., A*, 1993, **75**, 97–103.

7 K. Azrague, E. Bonnefille, V. Pradines, V. Pimienta, E. Oliveros, M.-T. Maurette and F. Benoit-Marquié, *Photochem. Photobiol. Sci.*, 2005, **4**, 406–408.

8 M. C. Gonzalez, E. Oliveros, M. Wörner and A. M. Braun, *J. Photochem. Photobiol., C*, 2004, **5**, 225–246.

9 G. V. Buxton and A. J. Elliot, *J. Chem. Soc., Faraday Trans.*, 1993, **89**, 485–488.

10 X.-Y. Yu, *J. Phys. Chem. Ref. Data*, 2004, **33**, 747–763.

11 B. H. J. Bielski, D. E. Cabelli, R. L. Arudi and A. B. Ross, *J. Phys. Chem. Ref. Data*, 1985, **14**, 1041–1100.

12 E. Arany, T. Oppenländer, K. Gajda-Schrantz and A. Dombi, Influence of H_2O_2 formed *in situ* on the photodegradation of ibuprofen and ketoprofen, *Curr. Phys. Chem.*, 2012, **2** [BSP/CPC/E-Pub/0013].

13 (*a*) G. Heit, A. Neuner, P.-Y. Saugy and A. M. Braun, *J. Phys. Chem. A*, 1998, **102**, 5551–5561; (*b*) G. Heit, *Optische in situ-Sauerstoffmessung, VUV-Aktinometrie und Numerische Simulation*, Dissertation, Fakultät für Chemieingenieurwesen und Verfahrenstechnik, Universität Karlsruhe (TH), Karlsruhe, 1996.

14 J. J. Wu, M. Muruganandham, L. T. Chang, G. J. Lee, V. N. Batalova and G. M. Mokrousov, *Ozone: Sci. Eng.*, 2011, **33**, 74–79.

15 G. Imoberdorf and M. Mohseni, *Chem. Eng. Sci.*, 2011, **66**, 1159–1167.

16 VDI 2468, Sheet 9, Messen der Wasserstoffperoxid-Konzentration, Registrierendes fluorimetrisches Verfahren, Verein Deutscher Ingenieure e.V. (VDI), Redaktion VDI-Richtlinien, Düsseldorf, 2005.

17 (*a*) M. C. Gonzalez and A. M. Braun, *J. Photochem. Photobiol., A*, 1996, **95**, 67–72; (*b*) M. C. Gonzalez, G. Carrillo Le Roux, J. A. Rosso and A. M. Braun, *Chemosphere*, 2007, **69**, 1238–1244.

18 (*a*) J. López Gejo, *Applications of the VUV-Photochemically Initiated Oxidation for Waste Gas Treatment and Surface Functionalization*, Dissertation, Fakultät für Chemieingenieurwesen und Verfahrenstechnik, Universität Karlsruhe (TH), Karlsruhe, 2005; (*b*) J. López-Gejo, H. Glieman, T. Schimmel and A. M. Braun, *Photochem. Photobiol.*, 2005, **81**, 777–782.

